International Journal of Nanoelectronics and Materials

In Press, Accepted Manuscript – Note to user

Observation of Blue Shift Absorption for Surface Plasmon Resonance in Gold Nano-islands

Abdulqader D. Faisal[1*], Mohammed O. Dawood[2], Khaleel I. Hassoon[1]

[1] Department of Applied Sciences, University of Technology, Baghdad, Iraq

[2] Department of Physics, College of Science, University of Mustansiriya, Baghdad, Iraq

ABSTRACT

Controllable and predefined absorption are essential in the synthesis of new optoelectronic devices. In this work, an ion coater unit with a modified chamber is used to sputter the gold nano-islands onto glass substrates. Empirical formula and field emission scanning electron microscope (FESEM) is utilized to estimate the nominal thicknesses of the nano-island. Atomic force microscopy (AFM) images showed low values of roughness for the ultrathin films. The FESEM reveals that most of the nano-islands have round shapes. The UV-VIS measurements demonstrated that gold nano-islands revealed two regimes of absorption. Moreover, the peaks of surface plasmon resonance, in particular, are shifted to longer wavelengths and broadened in width with an increased thickness from 12-120 nm. In reverse to this behavior, the peaks are blue shifted for nominal thicknesses lower than 12 nm. The enhanced absorption in the blue spectral region can be utilized to increase absorption in solid-state solar cells and enhanced the stimulated Raman scattering devices using predefined thickness and deposition parameters.

Keywords: Gold nanoparticles, Optical properties, Surface plasmon resonance, LSPR, Diode sputtering

1. INTRODUCTION

The field of nano-scale materials has attracted much attention in the last decades because of the need for new materials with novel properties [1-4]. In particular, nanostructures made from noble metals such as Au and Ag have enticed much interest because of their unique plasmonic properties in the visible region [5].

The application of electromagnetic theory to the optical properties of the metals was presented by Drude in 1894 [6]. This model had a good agreement with the experimental findings for only continuous thin films [7]. For ultrathin films, the optical properties were quite different from that of the bulk metal, and there was a remarkable unexplained change of the optical properties with thickness at that scale [7]. Garnett in 1904 [8] proposed that this change in the optical properties might be explained by postulating that the ultra-thin films were discontinuous in nature and could be composed of small aggregates or extremely fine islands and this fact has been also confirmed by electron microscope [7].

Corresponding author: abdulf330@gmail.com

Then, it was shown that the localized surface plasmon resonances (LSPR) of such nano-islands were playing an essential role in the optical properties.

In theory, the LSPR takes place when the free electrons are driven by the electric field of the electromagnetic waves in the nano-islands interact with the incident electromagnetic radiation [5]. Metallic nano-islands reveal different LSPR spectral locations and noble metals such as Au and Ag show strong absorption and scattering in the visible region [9]. The growth mechanism of these aggregates or islands was well-investigated by many earlier studies [10, 11]. Later on, other theoretical and numerical simulations were also implemented [12-16] to explain the optical properties of nano-islands deposited on different substrates. The optical response of the nano-islands was analyzed in many instances using what is called the effective-medium model [10, 17] or by calculation of polarizability of a truncated spheres and oblate spheroids in electrostatic approximation where an island size is considered much smaller than the wavelength of exciting light [12-16].

As it was reported in experimental studies, the plasmon resonance wavelength exhibited redshift with the increase of the nominal thickness of deposited films [10,11, 18,19]. Some researchers attributed this redshift to the differences in the nano-islands dimensions, the so-called aspect ratio [5,19,20]. In the present work, two groups of nominal thicknesses for Au nano-islands on glass substrate were prepared by diode sputtering technique. The first group with a small thickness is ranging from 2 to 12 nm, while the second with a large thickness is ranging from 12 to 120 nm, respectively. These two groups show different shifts (blue and red shifts) with the different range of nominal thickness. The observation of the blue shift in gold nano-islands is compatible with the UV shift observed in Ag nanoparticles [21].

2. EXPERIMENTAL METHOD

2.1 DC Diode sputtering chamber and re-designed holder

A schematic diagram of the working principle of the ion-coater is manifested in Fig.1a. The cylindrical glass chamber shown in Fig.1b has an outside diameter of 13.5 cm and a thickness of 8 mm. The cathode holder is covered with Teflon to carry the gold target with purity 99.99% and diameter 5 cm, as depicted in Fig.1b. The target-holder in that home-made chamber is modified so as to facilitate the holder to be moved up and down in order to vary the gap between the cathode and the anode. The holder is already fitted with aluminum flanges.

A target or any source of the material wanted to be deposited is bombarded with energetic ions of inert gas (typically argon ions, Ar^+). The active collisions between the ions and the target eject the atoms from the target into space. Then, the ejected atoms travel some distances until they reach the substrate where they condense into nano-islands.

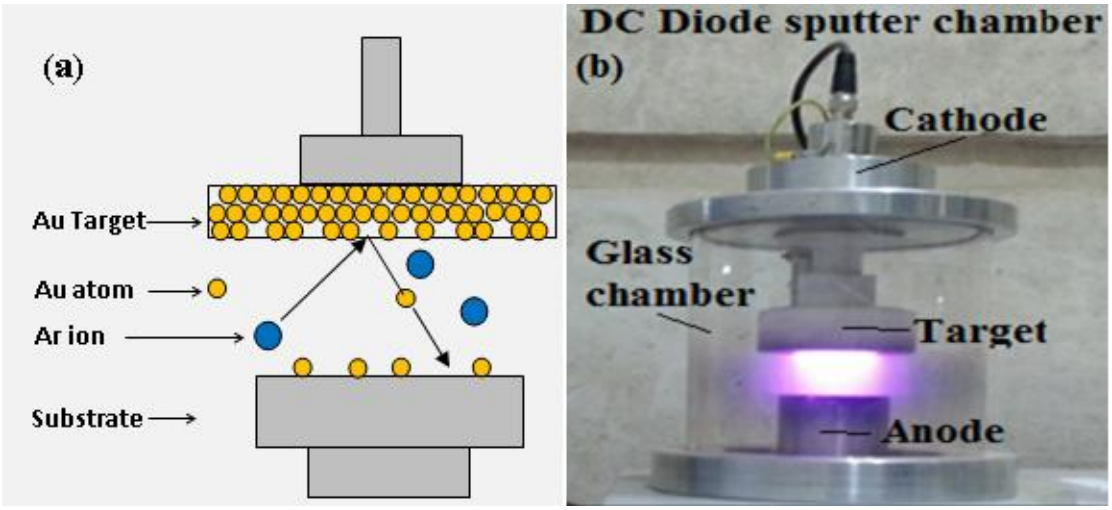

Figure 1. (a) Working principle of ion-coater **; (b)** Photograph of DC diode sputter chamber.

2.2 Gold sputtering on the glass substrate

Microscopic glass slides with sizes of 2.5 × 2.5 cm^2 and 1 mm thick were used as substrates. These substrates were first cleaned with soapy water, then with acetone and de-ionized water (DI water), and dried with nitrogen. The substrates were sonicated in acetone and methanol for 15 minutes, respectively. After that, they were rinsed again with DI water and finally blown with dry nitrogen. The chamber was evacuated by a rotary pump (Edwards) to sustain a low pressure. The sputter coater parameters and the deposition conditions are presented in Table 1. Moreover, Ar purity was 99.995%, a distance between electrodes was 3 cm. The sputtering time was varied from 5 to 600s.

Table 1 Sputtering parameters for Bio Rad Automatic Sputter Coater, Model E5200.

Base pressure	Working pressure	Flow rate	Applied voltage	Discharge power
0.02 mbar	0.15 mbar	150 sccm	1000 Volt	10 W

2.3 Film deposition and thickness measurements

The gold layer thickness was found from calculating the sputtering rate value which was determined using high sputtering time (600s). The experimental deposition rate was calculated to be 0.2 nm. s^{-1} for the present modified ion-coater system. Using this rate, the thickness can be inferred at any sputtering time. To confirm the thickness values of the current work, an empirical formula was also used which turned out to be (Ref. Manual guide for Bio-Rad Automatic Sputter Coater, Model E5200):

$$d(nm) = K \times I \times V \times t \quad (1)$$

K=0.017 is an experimentally determined constant for gold, I in mA unit is the ion current (20 mA), V in kV unit is the voltage (0.6 kV) and t in the second unit is the sputtering time. Figure 2 displays a calibration curve with a fitting value of sputtering rate equals to 0.2 nm. s^{-1}.

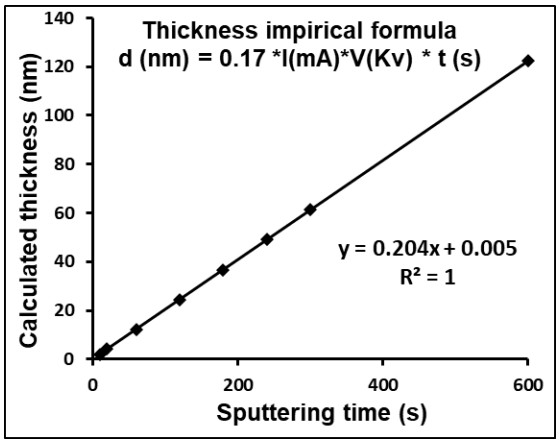

Figure 2. Gold film thickness calibration curve.

3. RESULTS AND DISCUSSION

3.1 AFM Imaging

Atomic force microscopy (AA3000 scanning probe microscope / SPM) was used to analyze the surface of the gold nanofilms sputtered on glass substrate. Figures 3 reveals the AFM images in 2D for typical gold nano-thin films sputtered on glass slides at various thicknesses and annealed at 500°C in the air for 4 hours. The images in this figure are scanned through x and y at sizes of (1.6µm x1.6µm). The surface roughness parameters are summarized in Table 2.

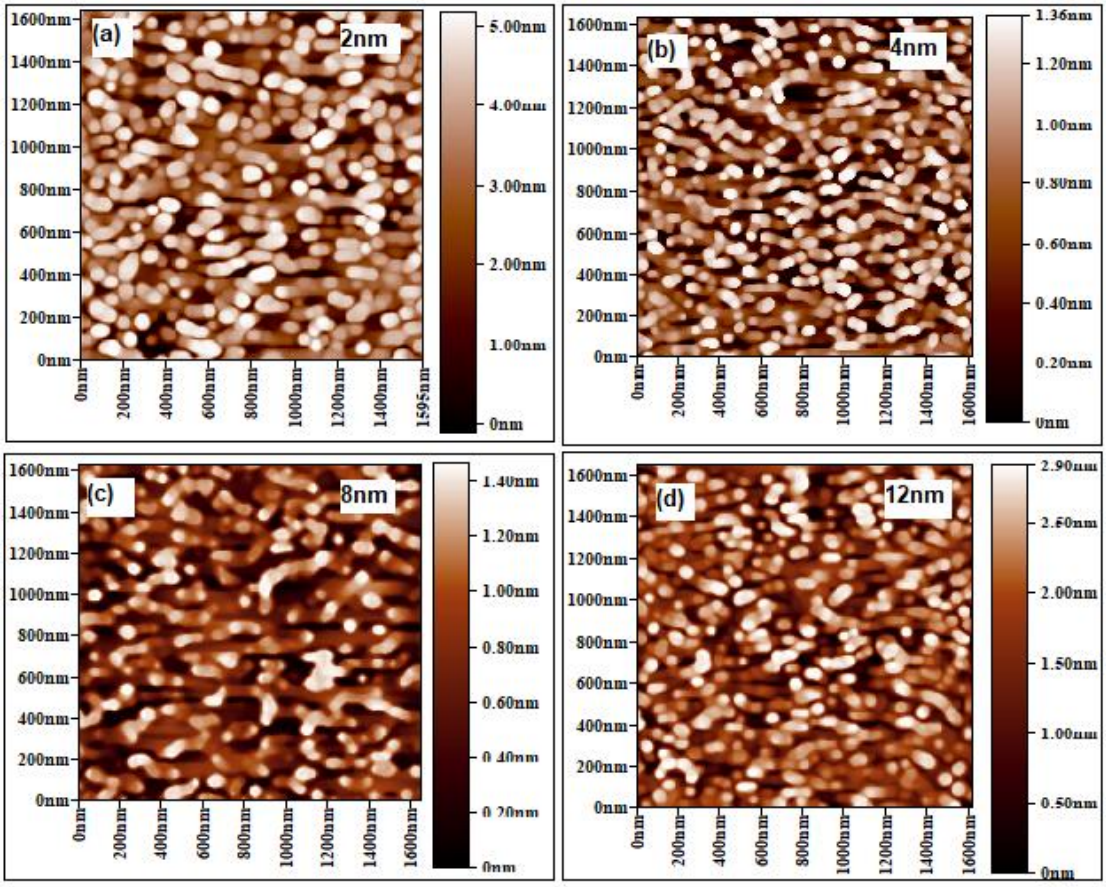

Figure 3. 2D AFM images for Au ultrathin films (a) 2 nm, (b) 4 nm, (c) 8 nm, and (d)12 nm thick gold sputtered film and annealed in air at 500°C for 4h in the air.

Table 2 AFM data for gold thin films prepared by diode sputtering.

Sample No.	Sputtering Time (sec.)	Gold Film Thickness (nm)	RMS Roughness (Sq) (nm)	Average Roughness (Sa)(nm)	Pk-Pk Roughness (nm)
S1	10	2	1.26	1.05	5.29
S2	20	4	0.369	0.317	1.36
S3	40	8	0.366	0.311	1.44
S4	60	12	0.656	0.545	2.9
S5	120	24	4.33	3.71	16.8
S6	240	48	0.677	0.568	2.58

3.2 FESEM Imaging

Field emission scanning electron microscopy (FESEM) was used to identify the topography of the samples prepared by ion coater and also to confirm the values of nominal thicknesses calculated by Eq.(1) using cross-sectional imaging. Figure 4 exhibits three FESEM images of gold nano-thin films at various thicknesses (48, 60, 120 nm) deposited at a constant rate of 0.2 nm. s^{-1}. It is well-known that the metal nanoparticles do not wet the glass surface and their growth follows the growth mechanism of Volmer-Weber growth [22,23]. At the beginning of the deposition process the atoms tend to coalesce into isolated nanoparticles with spherical or semi-spherical shapes. Figure 4(a-c) shows the isolated nano-islands with a nominal thickness of 48, 60, and 120 nm, respectively. In general, the nano-islands are not uniform in size or shape but most of them tend to take a round shape. Their size slightly increases with a nominal thickness of 48-120 nm. In Fig. 4(a-c), the film has a grain size of about 30.5, 31 nm and 33 nm, respectively. In particular, the nanoparticles in Fig. 4a is more distributed in size and the film is highly discontinuous.

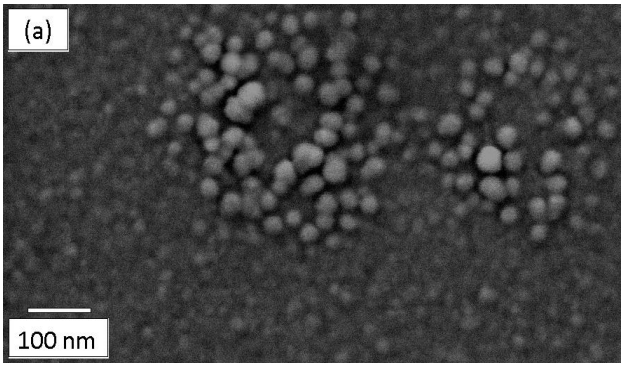

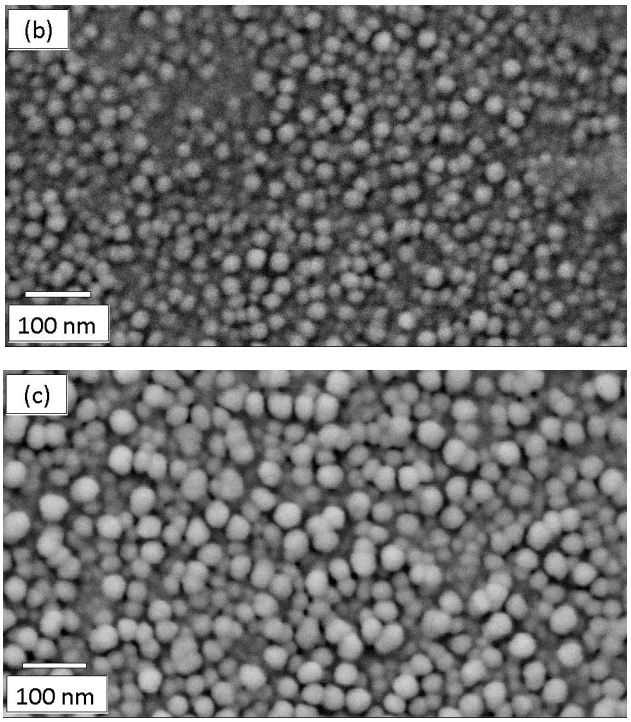

Figure 4. SEM images showing the topography of Au nano-islands and nano-films deposited on glass substrates. Nominal thickness is (a) 48 nm (b) 60 nm (c) 120 nm.

3.3 XRD Analysis

The x-ray diffraction technique (XRD- Shimadzu 6000/ Japan) was used to investigate the crystal structure of a typical gold sputtered on a glass with a thickness of 120 nm followed by annealing in air at 500ºC for 4h. Figure 5 shows the diffraction peaks at 2θº =38.2º, 44.4º, 64.6º and 77.6º which they are corresponding to the reflection planes of (111), (200), (220) and (311) respectively. These are indicating that the Au film is pure crystalline according to the crystallography Open Data (COD) card No.96-900-8464. The XRD spectrum displays a very intense peak at (111), which is attributed to the well oriented single crystal of gold along [111].

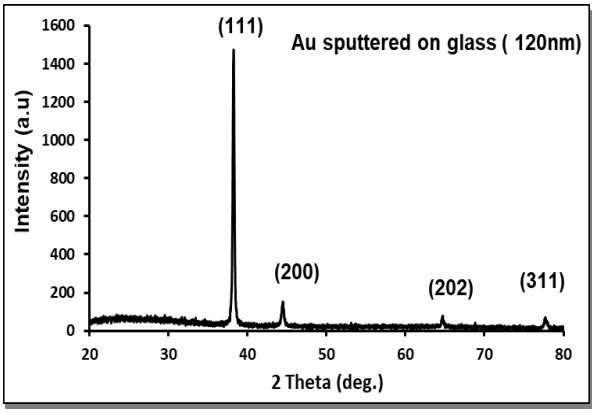

Figure 5. XRD pattern for 120 nm gold film sputtered on a glass and then annealed in air at 500°C for 5h.

The crystallite size of the gold nanostructures was calculated via Scherrer's formula [24]:

$$D = \frac{0.9\lambda}{\beta \cos\theta} \tag{2}$$

where D is the grain size (nm), λ is the wavelength, β is the half width at half maximum (HWHM) and θ is the Bragg's diffraction angle. Figure evinces that the crystallite size of the gold film is varied relative to the thickness, where the data has a grain size (nm) given by a power law fitting:

$$D = ct^{\alpha} \tag{3}$$

where c is the proportionality constant (c =49 for our sputtering chamber), t is the gold film thickness and α is a power factor (for gold $\alpha \approx 0.18$). The structural parameters are listed in Table 3.

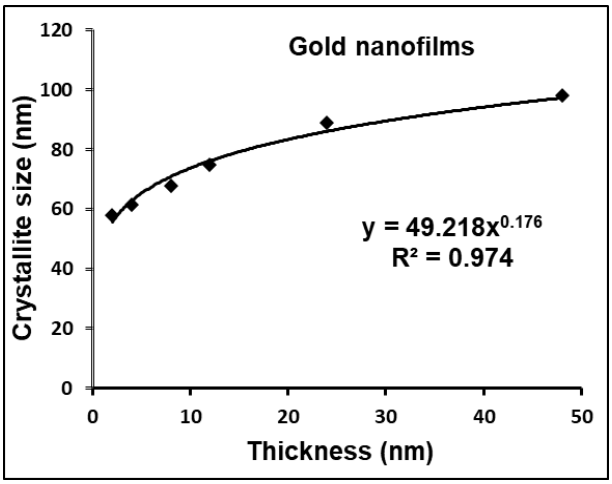

Figure 6. Crystallite size as a function of nominal thickness.

Table 3 XRD data for 120 nm Au sputtered on glass

Present work				COD card # 96-900-8464
2θº	d (Å)	Reflection plane	Crystallite size (nm)	d (Å)
38.2	2.3528	(111)	36.5	2.3546
44.4	2.0372	(200)	28.9	2.0391
64.6	1.4409	(220)	31.6	1.4419
77.6	1.2289	(311)	37.78	1.2296

3.4 OPTICAL PROPERTIES

The optical absorption of Au nanoparticles for wavelength from 300 to 1000 nm was measured using UV-VIS spectrophotometer (UV-2800). The photographs in Fig.7a reveal how the appearance of gold thin films is varied with the large thicknesses before and after annealing, and Fig.7b represents the small thicknesses. Figure 8a and 8b demonstrate the absorption spectra of the gold nano-structured prepared by the sputtering technique for the large thicknesses 12-120 nm and for the small thicknesses,

respectively. All the films show two absorption peaks that correspond respectively to interband and plasmonic transitions. For thicknesses 24-120 nm shown in Fig.9a, the plasmonic peaks clearly shift to higher wavelength side (redshift) with increasing thickness of Au thin films. However, for the lower thicknesses 4, 8 and 12 nm clarified in Fig.9b, the plasmonic peaks shift to lower wavelengths.

It is well-known that the gold nanoparticles with spherical shapes reveal only one peak belongs to LSPR, which shifts to higher wavelength's side (redshift) and expands in width with an increase in their particle size [3]. However, the gold nanoparticles deposited on glass substrates shows two recognizable peaks. The position and width of each peak have thickness dependency. The peaks in Figure 8a with diameters greater than 12 nm are red shifted where the role of phase retardation effects are dominated [25]. On the other hand, the peaks in Figure 8b with diameters less than 12 nm, known as the intrinsic size region [3] or the quasi-static regime are blue shifted where the quantum confinement effect becomes predominant. The redshift is compatible with earlier results on gold nano-islands prepared by thermal evaporation [9].

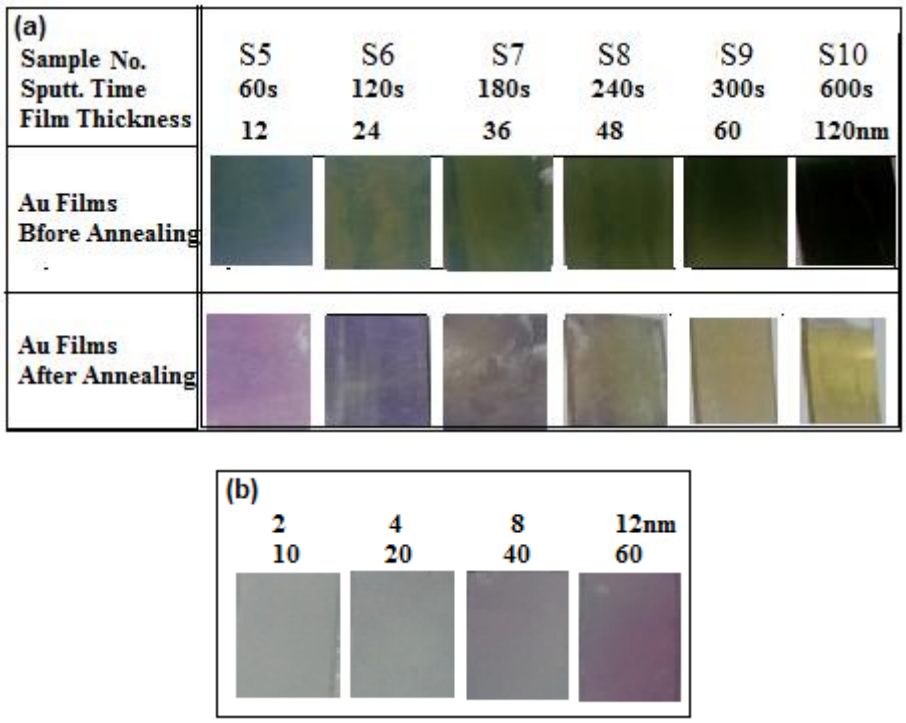

Figure 7. Photograph of gold films sputtered on glass substrates before and after annealing for large thickness (a) and for small thickness (b).

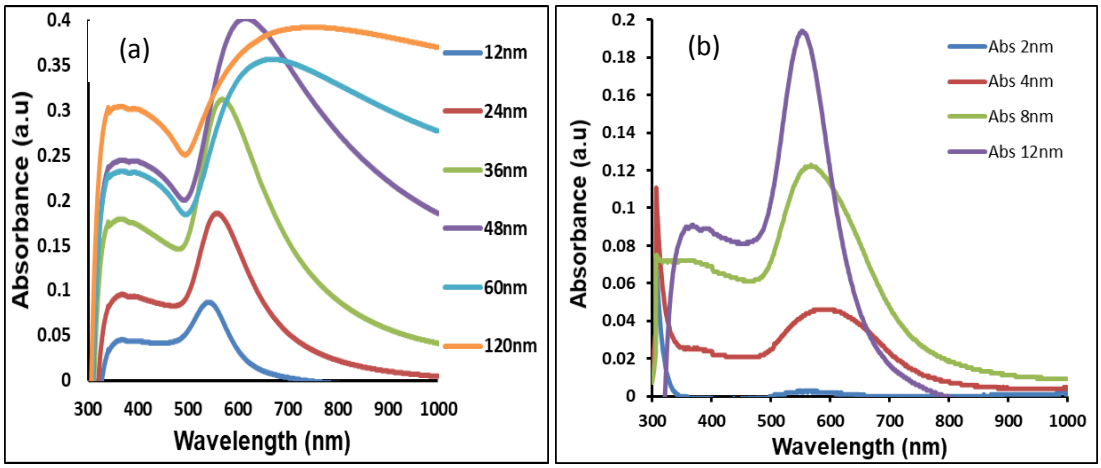

Figure 8. UV-Visible absorption spectra versus wavelength at various times of sputtering. Absorption spectra of the gold film of large thicknesses (a) and small thicknesses (b).

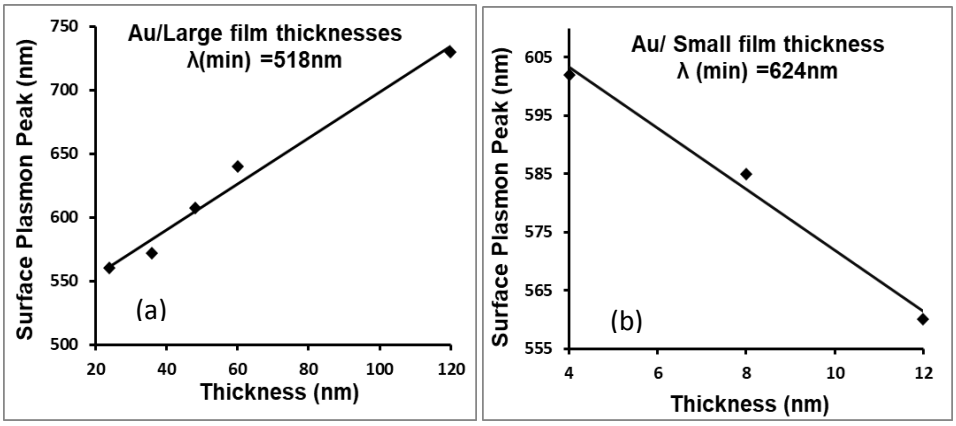

Figure 9. Variation in the peak position of surface plasmon resonance for (a) large thicknesses and (b) small thicknesses.

CONCLUSION

Gold thin films with nominal thickness in the range from 2 to 120 nm were deposited onto glass substrates via sputtering technique and annealed in air at the temperature of 500ºC for 4h. Besides being red shifted for thicknesses higher than 12 nm, the absorption peaks are blue shifted for thicknesses lower than 12 nm. This type of ultra-thin films can be used as functional materials because their optical properties have a thickness dependency. Keeping in mind that the Au nanoparticles are active generators of hot carriers [26], and the optical properties can be modified using a different substrate material such as TiO_2 [27], these unique features could have in the future great impact on the fabrication of solid-state solar cells and enhanced stimulated Raman scattering devices.

REFERENCES

[1] Sodipo, B.K., Abdul Aziz, A., Mustapa, M., 2015. Int. J. Nano electron. and Mater. 8, 1-6.
[2] Fouad, S., Sabri, N., Jamal, Z.A.Z., Poopalan, P., 2017. Int. J. Nano electron. and Mater. 10, 149-158.
[3] Stephan, L., Mostafa, A.E., 1999. J. Phys. Chem. B 103, 8410-8425.

[4] Abdulmunem, O., Hassoon,K., Gaafar, M., Rahimi-Iman, A., Balzer, J., 2017. J. Infrared Millim. Te. 38, 1206-1214.
[5] Alexander, Boris, A., Gady, G., 2013. Opt. Express 21, 4126-4138.
[6] W.A. Neil, M. David, Solid State Physics, ed., Holt, Rinehart and Winston, New York 1976.
[7] Sennett, R.S., Scott, D.G., 1950. J. Opt. Soc. Amerca, 40, 203-211.
[8] Maxwell, G.J.C., 1904. Phil. Trans. R. Soc. Lond. A 203, 385-420.
[9] Rai, V.N., Srivastava, A.K., Mukherjee, C., Deb, S.K., 2014. arXiv preprint arXiv:1406.4605.
[10] Norman, T.A., Granqvist, C.G., 1978. Phys. Rev. B 18 647-695.
[11] Norrman, S., Andersson, T., Granqvist, C.G., Hunderi, O., 1977. Solid State Commun. 23 261-265.
[12] Wind, M.M., Vlieger, J., Bedeaux, D., 1987. Physica A 141, 33-37.
[13] Wind, M.M., Bobbert, P.A., Vlieger, J., Bedeaux, D., 1987. Physica A 143, 164-182.
[14] Wind, M.M., Bobbert, P.A., J. Vlieger, Bedeaux, D., 1988. Thin Solid Films 164, 57-62.
[15] Wind, M.M., Bobbert, P.A., Vlieger, J., Bedeaux, D., 1989. Physica A 157, 269-278.
[16] Simonsen, I., Lazzari, R., Jupille, J., Roux, S., 2000. Phys. Rev. B 61, 7722-7733.
[17] Granqvist, G.G., Hunderi, O., 1977. Phys. Rev. B 16, 3513-3534.
[18] Amendola, V., Pilot, R., Frasconi, M., Maragò, O.M., Iatì, M.A., 2017. J. Phys.: Condens. Matter. 29, 203002 (48pp).
[19] Gotschy W, Vonmetz, K, Leitner, A., Aussenegg, F.R., 1996. Appl. Phys. B 63, 381-384.
[20] Kelly, K.L. Coronado, E., Zhao, L.L, Schatz, G.G., 2003. J. Phys. Chem. B 107, 668-677.
[21] Raza, S., Stenger, N., Kadkhodazadeh, S., Fischer, S.V., Kostesha, N., Jauho, , A.P., Burrows, A., Wubs, M., Mortensen, N.A., 2013. Nanoph, 2(2), 131-138.
[22] Fedorovich, R., Naumovets, A.,Tomchuk, P., 2000, Phys. Rep. 328, 73-179.
[23] Wei, H., Eilers, H., 2009 J. Phys. Chem. Solids 70 (2), 459-465.
[24] A. Guiner, X-ray diffraction in crystals, imperfect crystals and amorphous bodies. Reprint of the W. H. Freeman & Company, San Francisco, 1963.
[25] Su, K.H., Wei, Q.H., Zhang, X., Mock, J.J., Smith, D.R., Schultz, S., 2003. Nano Lett. 3, 1087-1090.
[26] Forno, D., Ranno, S., Lischner, J., 2018. J. Phys. Chem. C, 122(15), 8517-8527.
[27] Yao, ., Liu, Q.L., Zhao, Z.Y., 2018. Catalysts, 8, 236-251.